Z. Phys. B 101, 597–611 (1996)

ZEITSCHRIFT
FÜR PHYSIK B

The one-dimensional ANNNI model in a transverse field: analytic and numerical study of effective Hamiltonians

Heiko Rieger[1,2], **Genadi Uimin**[1,3]

[1] Institut für Theoretische Physik, Universität zu Köln, D-50937 Köln, Germany
[2] HLRZ, Forschungszentrum Jülich, D-52425 Jülich, Germany
[3] Landau Institute for Theoretical Physics, Chernogolovka, Moscow District, Russia

Received: 20 March 1996

Abstract. We consider a quantum spin-$\frac{1}{2}$ Ising chain with competing nearest and next-nearest neighbor interactions in a transverse magnetic field, which is known to be equivalent to the classical two-dimensional ANNNI model. Within a perturbation theory for small transverse field (corresponding to low temperatures in the classical ANNNI model) we derive two effective Hamiltonians: the free model describing free fermions on a fictitious lattice that excludes particular heavy excitations of the original system; and the complete model, which incorporates creation and annihilation of these fermions. Whereas the former possesses only three phases (ferromagnetic, floating and anti phase), the latter contains the full physics of the 2d ANNNI model, including a paramagnetic phase between the ferromagnetic and floating phase and a Kosterlitz-Thouless transition. New analytic results are derived for the free model, e.g. the excitation spectrum that turns out to be non-trivial. Our effective Hamiltonians are defined on a restricted Hilbert space so that exact diagonalization calculations can be done for much larger system sizes. Results from extensive Lanczos calculations for system sizes up to $L = 32$ are presented confirming the original predictions from Villain and Bak.

PACS: 05.30.Fk; 75.10.Jm; 75.40.Mg

I. Introduction

Frustrated Ising models in a transverse field have been investigated for a long time [1]. The transverse field plays the role of a tunable parameter by which one can induce a so called "quantum phase transition" at zero temperature that is driven by quantum fluctuation alone [2] (as opposed to a conventional, thermally driven phase transition). Frustration can be introduced via disorder, as for example in the case of quantum Ising spin glasses that have gained much interest quite recently [3]. However, it can also be produced in a regular fashion as e.g. in the anisotropic next nearest neighbor Ising model (ANNNI) [4], where competing nearest and next-nearest neighbor interactions are the origin of the richness of the phase diagram. This is the model that we intend to re-investigate in this paper. To be concrete, we consider the Hamiltonian, $\mathscr{H}$, of a $1d$ spin-$\frac{1}{2}$ chain in a transverse magnetic field, which consists of the two parts: the classical $1d$ ANNNI model plus quantum fluctuations imposed by transverse field:

$$\mathscr{H} = H_{\mathrm{cl}} + H_{\mathrm{qu}}, \tag{1}$$

$$H_{\mathrm{cl}} = -\mathscr{J}\sum_i \sigma_i^z \sigma_{i+1}^z + \kappa\mathscr{J}\sum_i \sigma_i^z \sigma_{i+2}^z \quad \text{and}$$

$$H_{\mathrm{qu}} = -\Gamma\sum_i \sigma_i^x \tag{2}$$

$\Gamma = 0$ corresponds to a classical ANNNI model in which $\mathscr{J}$ is supposed to be positive. σ^z and σ^x are the Pauli matrices:

$$\sigma^z = \begin{pmatrix} 1 & 0 \\ 0 & -1 \end{pmatrix}, \quad \sigma^x = \begin{pmatrix} 0 & 1 \\ 1 & 0 \end{pmatrix} \tag{3}$$

The most interesting region of this model is the region around $\kappa = 1/2$. The classical part H_{cl} has an infinite ground state degeneracy at this point, separating the ferromagnetic (FM) region ($\kappa < 1/2$), where the ground-state is given by "all-spins-up" or "all-spins-down", from the anti-phase region ($\kappa > 1/2$), where the ground-state has a period 4 with two down-spins following two up-spins. After [6] $\langle 2 \rangle$ is a traditional notation for this anti-phase. Switching on the quantum fluctuations via a nonvanishing transverse field induces the presence of different phases: fixing $\Gamma \ll J$ and increasing κ in the vicinity of 1/2, one can distinguish

- FM ($\langle \sigma_i^z \rangle \neq 0$);
- PM, i.e., paramagnetic phase (exponentially decaying spatial spin-spin correlations, no long-range order);
- FP, i.e., floating phase (algebraically decaying spatial spin-spin correlations, accompanied with a modulation continuously changed with κ, no long-range order);
- $\langle 2 \rangle$ ($\langle \sigma_i^z \sigma_{i+2}^z \rangle < 0$, $\langle \sigma_i^z \sigma_{i+4}^z \rangle > 0$).

The FM-PM transition is well understood: It is within the same universality class as the two-dimensional Ising model or 1d unfrustrated Ising model in a transverse field (see, e.g., [7, 8]).

Villain and Bak [9] in their seminal work on the two-dimensional ANNNI model argued that the $\langle 2\rangle$-FP transition is expected to be of the Prokovsky-Talapov type [10] and that the FP-PM transition is expected to be of the Kosterlitz-Thouless type [11]. Since this work is based on various plausible but not rigorously proven assumptions many attempts have been done to check these predictions with Monte Carlo simulations or exact diagonalization studies (for a review see [4]). However, for principle reason that we also try to clarify in this paper, such an endeavor turns out to be very difficult and fails to provide the theory either with a conclusive support or with a clear falsification.

A principal question of this work is how to catch the essential physics in the vicinity of the FP–$\langle 2\rangle$ and FP-PM transitions. For doing this we present a regular expansion of Hamiltonian (1) in powers $\Gamma/\mathscr{J}$, which allows to perform exact numerical diagonalization for longer chains than it is possible to achieve by a straightforward procedure.

The organization of the paper is as follows: In Sect. II we recapitulate the free fermion picture of Villain and Bak [9] before we present the above mentioned effective Hamiltonian. Then in Sect. III we compare the analytical predictions of this theory for *finite* systems with the results of exact diagonalization studies and proceed to extract the desired information about the critical behavior. Section IV summarizes our results.

II. Free fermion picture

Near $\kappa = 1/2$ the elementary excitations can be distinguished as light and heavy. The main idea is to map the initial Hamiltonian onto the states where the heavy excitations are excluded from.

We start with a conditional FM vacuum state, for example, .. + + + + + .., then the excitation with an isolated (−) spin, e.g., .. + + − + + .. costs the energy $4\mathscr{J}(1-\kappa)$ which is not small as $\kappa \to 1/2$. However, the excitation with two or more sequential spins rotated, e.g., .. + + − − + + .. costs the energy $4\mathscr{J}(1-2\kappa)$ which vanishes with $\kappa - 1/2$. At the next step we can introduce quasiparticles, which are the domain walls (DW's) defined on the *dual* lattice. The latter coincides in $1d$ with the middles of the links. The energy of a single DW, i.e., .. + + + $\overset{\text{dw}}{|}$ − − − .., is determined by the classical part of $\mathscr{H}$:

$$\varepsilon = 2\mathscr{J}(1-2\kappa). \tag{4}$$

The DW's which occupy the nearest sites of the dual lattice repel each other with the cost of energy $V = 4\mathscr{J}\kappa$. In general any state now is characterized by positions of the DW's on the dual lattice

$$\{\ell_1, \ell_2, \ldots, \ell_k\}. \tag{5}$$

For convenience we set the coordinates on a dual lattice to be integer numbers, $1, \ldots, L$, while the sites of a real lattice run half-integer numbers, say, $1/2, \ldots, L-1/2$. The quantum part of $\mathscr{H}$ plays a role of the kinetic energy of quasiparticles. In fact, applying H_{qu} to the state with a DW located at the site ℓ, the spin from either its right or its left is changed by sign, that means a shift of a DW by one unit. Applying H_{qu} to the site with no DW's surrounding it creates a couple of DW's. Hermitian conjugation corresponds to annihilation of those DW's.

All the matrix elements described in terms of DW variables on the dual lattice can be summarized in the following Hamiltonian:

$$\mathscr{H} = H_0 + H_1, \quad H_0 = V\sum_j n_j^{(\tau)} n_{j+1}^{(\tau)}$$
$$H_1 = \varepsilon\sum_j n_j^{(\tau)} - \Gamma\sum_j (\tau_j^+\tau_{j+1}^+ + \tau_j^-\tau_{j+1}^- + \tau_j^+\tau_{j+1}^- + \tau_j^-\tau_{j+1}^+) \tag{6}$$

where τ's are usual Pauli matrices and $n^{(\tau)} = (1-\tau^z)/2$. A conditional vacuum is a state with no DW's ($\tau_j^z = 1$ or $n_j^{(\tau)} = 0$ in (6)), creation (annihilation) of a DW is realized by τ^- (τ^+). A standard derivation of Hamiltonian (6) and transformation from spin-operators σ's to spin-operators τ's is given in Appendix A.

A routine procedure of the Jordan-Wigner transformation

$$\tau_j^+ = c_j \exp\left(\pi\sum_{k=1}^{j-1} n_k\right)$$

allows to deal with fermionic variables. Below we shall use the periodic boundary conditions, that means that the $L+1$-th site should be identified with the first. Hamiltonian (6) can be rewritten now as

$$\mathscr{H} = \sum_{j=1}^{L-1} (\varepsilon n_j + V n_j n_{j+1} - \Gamma(c_j^\dagger c_{j+1}^\dagger + c_{j+1}c_j + c_j^\dagger c_{j+1} + c_{j+1}^\dagger c_j)) + V n_1 n_L - \Gamma(c_1^\dagger c_L^\dagger + c_L c_1 - c_1^\dagger c_L - c_L^\dagger c_1)\exp(i\pi k) \tag{7}$$

where $k = \sum_1^L n_j$, a total number of DW's. Evidently, k should be even number on a cyclic chain that results in $\exp(\pi k) \equiv 1$.

Assuming $V \gg (\varepsilon, \Gamma)$ one can obtain the effective Hamiltonian, $\mathscr{H}_{\text{eff}}^{(1)}$, which reflects low energy properties of $\mathscr{H}$ with the energy scale of order (ε, Γ). Note, that the V-term makes two DW's energetically unfavorable if they occupy the nearest sites. Simultaneously, terms $\Gamma(\tau^+\tau^+ + \tau^-\tau^-)$ of (6) (or terms $\Gamma(c^\dagger c^\dagger + cc)$ of (7)) should be excluded from the effective Hamiltonian, which now reads in τ-variables

$$\mathscr{H}_{\text{eff}}^{(1)} = \sum_{j=1}^{L-1} (\varepsilon n_j^{(\tau)} - \Gamma(\tau_j^+\tau_{j+1}^- + \tau_j^-\tau_{j+1}^+)) - \Gamma(\tau_1^+\tau_{\text{L}}^- + \tau_1^-\tau_{\text{L}}^+) \tag{8}$$

and in fermionic variables

$$\mathscr{H}_{\text{eff}}^{(1)} = \sum_{j=1}^{L-1} (\varepsilon n_j - \Gamma(c_j^\dagger c_{j+1} + c_{j+1}^\dagger c_j)) + \Gamma(c_1^\dagger c_{\text{L}} + c_{\text{L}}^\dagger c_1). \tag{9}$$

The constraint should be imposed on a possible wave function: DW's, or fermions, occupying the nearest sites, are forbidden.

Let us try a wave function of the form

$$\psi = \sum_{m_1} \dots \sum_{m_k} f(m_1, m_2, \dots, m_k) c^{\dagger}_{m_1} c^{\dagger}_{m_2} \dots c^{\dagger}_{m_k} \tag{10}$$

where k should be even. We may search for the amplitudes f's in a form of Bethe substitution:

$$f(m_1, m_2, \dots, m_k) = \sum_{\{P\}} \xi_{\mathrm{P}} \exp \imath (q_{P_1} m_1 + \dots + q_{P_k} m_k) \tag{11}$$

where $\{P\}$ is a permutation of numbers $\{1, 2, \dots, k\}$. Using the results of Appendix B we obtain a general expression for the eigenfunctions of Hamiltonian (7) in the $V \to \infty$ limit

$$\psi = \sum_{m_1} \dots \sum_{m_k} \begin{vmatrix} e^{\imath q_1 m_1} & e^{\imath q_1 (m_2 - 1)} & \dots & e^{\imath q_1 (m_k - k + 1)} \\ e^{\imath q_2 m_1} & e^{\imath q_2 (m_2 - 1)} & \dots & e^{\imath q_2 (m_k - k + 1)} \\ \dots & \dots & \dots & \dots \\ e^{\imath q_k m_1} & e^{\imath q_k (m_2 - 1)} & \dots & e^{\imath q_k (m_k - k + 1)} \end{vmatrix}$$

$$c^{\dagger}_{m_1} c^{\dagger}_{m_2} \dots c^{\dagger}_{m_k} |0\rangle. \tag{12}$$

The wave function (12) can be interpreted as a wave function of a tight-binding fermion model on a fictitious lattice. The coordinate of a fermion in a fictitious lattice coincides with that one in a real lattice minus the number of fermions situated from its left. We shall also use another interpretation which will be convenient in numerical diagonalization. It is consistent with introducing two kind of "particles", $\mathscr{A}$ and $\mathscr{B}$. $\mathscr{A}$ is composed of a DW (or fermion) with a nearest empty site from its right attached. $\mathscr{B}$ represents an empty site which has no a nearest DW from its left. The $\mathscr{A}$–$\mathscr{B}$ representation will be discussed in Sect. III in detail.

The ground state energy of any intermediate state on the phase diagram between the FM and $\langle 2 \rangle$ boundaries

$$E_{\mathrm{gs}} = k\varepsilon - 4\Gamma \sum_{m=1}^{k/2} \cos \frac{(2m-1)\pi}{L-k} = k\varepsilon - 2\Gamma \frac{\sin \pi k/(L-k)}{\sin \pi/(L-k)} \tag{13}$$

is a function of k, the total amount of DW's, which characterizes modulation of a spin structure. Equation (13) describes the ground-state energies of the FM structure ($k = 0, E_{\mathrm{gs}} = 0$) and of the $\langle 2 \rangle$ structure ($k = L/2, E_{\mathrm{gs}} = L\varepsilon/2$) as well. Both structures, FM and $\langle 2 \rangle$, can be unstable with respect to formation either DW's ($k = 2$) or "holes" in a regular DW structure ($k = L/2 - 2$) [12]

For a finite cyclic chain we determine the boundaries from equations:

- FM–FP: $\varepsilon = 2\Gamma \cos \dfrac{\pi}{L-2} \overset{L \to \infty}{\Rightarrow} 2\Gamma$

$\langle 2 \rangle$–FP: $\varepsilon = -2\Gamma \left(\cos \dfrac{2\pi}{L} + 4 + \cos \dfrac{6\pi}{L+4} \right) \overset{L \to \infty}{\Rightarrow} -4\Gamma$

For an infinite chain we may introduce $q = \lim_{L \to \infty} k/L$, the concentration of DW's, which may be varied from 0 to 1/2. The analogue of (13) in the limit $L \to \infty$

$$\frac{E_{\mathrm{gs}}}{L} = q\epsilon - 2(1-q)\Gamma \int_0^{k_F} \frac{\mathrm{d}k}{\pi} \cos k \tag{14}$$

where $k_F = \pi q/(1-q)$. Differentiating over q in (14) shows how q changes with ε/Γ [9]:

$$\frac{\varepsilon}{\Gamma} = -\frac{1}{\pi} \sin k_\Gamma + \frac{1}{1-q} \cos k_F. \tag{15}$$

The first excited states whose energies are numerically calculated in Sect. III are non-trivial even in the framework of the free fermionic approach (cf Eqs. (C.3) and (C.4)). In Appendix C we derive Eq. (C.2) for the energy $\Delta E(Q)$ as a function of the wavevector Q. Such a fermion-hole excitation leaves the DW number unchanged. It becomes gapless at certain Q's when $L \to \infty$. In this limit the only non-zero contribution to $\Delta E(Q)$ is given by Eq. (C.5):

$$\Delta E(Q) = 4 \sin x \cdot \begin{cases} |\sin(x - k_{\mathrm{F}})|, & 0 < x < \pi/2 \\ |\sin(x + k_{\mathrm{F}})|, & \pi/2 < x < \pi \end{cases};$$

$$x = \frac{|Q|}{2} \left(1 + \frac{k_{\mathrm{F}}}{\pi} \right) \tag{16}$$

which is shown for $k_{\mathrm{F}} < \pi/2$ in Fig. 1. If $k_{\mathrm{F}} > \pi/2$ one has to substitute $\pi - k_F$ for k_F. The fermion-hole excitation plot is symmetric when a momentum transfer, Q, changes from 0 to $2k_F(1 + k_F/\pi)^{-1}$. It formally differs of the results predicted by Eqs. (C.3) and (C.4). These occur due to a contribution of order $1/L$ in the first two terms in the r.h.s. of Eq. (C.2). However, this contribution is still important when the finite-size systems are analyzed.

This is noteworthy, that the contraction of the wavevector, $2k_F \to 2k_F(1 + k_F/\pi)^{-1}$, when a fermion is transfered from one Fermi-point to another, can be attributed to strong "anti"-correlated properties of our spinless "free" fermions, that forces for using a fictitious lattice description.

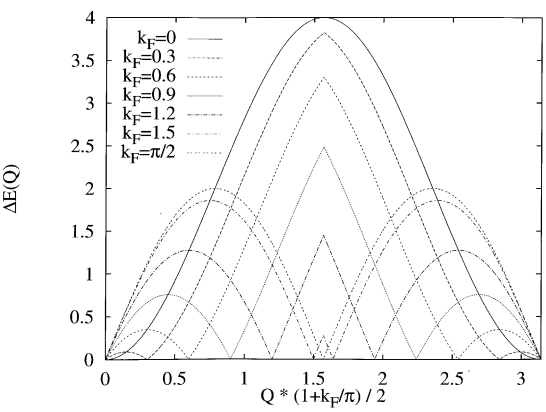

Fig. 1. The one particle excitation energy $\Delta E(\mathrm{Q})$ for the free model from (13) versus the contracted wave vector $Q \cdot (1 + k_F/\pi)/2$ for different values of $k_F = \pi q/(1-q)$, with q the domain wall density (which can be evaluated as a function of κ and Γ/J via equation (15)). $k_F = 0$ corresponds to the FM-phase, $k_F = \pi/2$ corresponds to $q = 1/3$, and for k_F between $\pi/2$ and π ($q = 1/2$, i.e. $\langle 2 \rangle$-phase) the evolution is simply reversed

As has been shown in [9] the FP should exhibit a power-like decay of correlation functions, e.g.,

$$\langle \sigma_i^z \sigma_{i+r}^z \rangle \propto r^{-\rho} \cos(\pi q r) \tag{17}$$

with $\rho = (1-q)^2/2$. This q-dependent ρ is also a result of the fictitious lattice contraction which increases with q. However, the FP cannot cover the whole range $0 < q < 1/2$: within the free model it becomes unstable at smaller q's and transforms into the PM state through the mechanism of the Kosterlitz-Thouless transition at $\rho = 1/4$[9], corresponding to a wavevector

$$q_{\mathrm{PM-FP}} = 1 - 1/\sqrt{2} \approx 0.292 \tag{18}$$

In the complete model this estimate holds only approximately, with increasing accuracy for decreasing Γ/J.

Hamiltonian (6) allows to go beyond the first order in Γ which has been discussed above. A non-trivial contribution in the second order in Γ to perturbation theory results in appearance the terms, which create (annihilate) DW's on next nearest sites. In fact, a couple of DW's on the sites, say, j and $j+2$, can be created as a two-step process: First, if the high-energy excitation is virtually created by $\tau_j^+ \tau_{j+1}^+$, then a many-fold degenerated ground state can be restored by $\tau_{j+1}^- \tau_{j+2}^+$. The second possibility is in a sequential process: $\tau_{j+1}^+ \tau_{j+2}^+$ and $\tau_{j+1}^- \tau_j^+$. Perturbation theory in the Γ^2-order also extends the DW hopping terms up to next nearest neighbors, but this extension is out of relevance.

Thus, in addition to Hamiltonian (8) we obtain

$$\mathscr{H}_{\mathrm{eff}}^{(2)} = -\gamma \left(\sum_{j=1}^{L-2} \tau_j^+ \tau_{j+2}^+ + \tau_1^+ \tau_{L-1}^+ + \tau_2^+ \tau_L^+ + \mathrm{HC} \right) \tag{19}$$

which can be also written in terms of fermions:

$$\mathscr{H}_{\mathrm{eff}}^{(2)} = -\gamma \left(\sum_{j=1}^{L-2} c_j^\dagger c_{j+2}^\dagger + c_1^\dagger c_{L-1}^\dagger + c_2^\dagger c_L^\dagger + \mathrm{HC} \right) \tag{20}$$

We put $\gamma = 2\Gamma^2/V$ in (19)–(20) and HC denotes Hermitian conjugate.

In spite of a smallness of $\mathscr{H}_{\mathrm{eff}}^{(2)}$ as compared to $\mathscr{H}_{\mathrm{eff}}^{(1)}$ the former significantly influences on the critical properties of the FP: $\mathscr{H}_{\mathrm{eff}}^{(2)}$ forces the FM–FP transition to be of the Ising type and transforms this, in fact, into the FM–PM. This results in a gap opening in the PM phase. The excitation spectrum in a low DW density limit behaves as (k here is the wavevector)

$$\sqrt{(\varepsilon - 2\Gamma\cos k)^2 + (2\gamma \sin k)^2} \tag{21}$$

which remains of a single-minimum kind within a narrow interval $2\Gamma < \varepsilon < 2\Gamma - 2\gamma^2/\Gamma$, then it develops in a double-minimum curve. The gap value, in general, is $\propto \Gamma^2$

The situation on the FP $-$ $\langle 2 \rangle$ boundary is different: This state is characterized by a regular DW structure and elementary excitations driven by $\mathscr{H}_{\mathrm{eff}}^{(2)}$ are the four -"leg" dislocations, which must be irrelevant [13]. This "leg"-number can be easily illustrated in terms of the $\mathscr{A}$ and $\mathscr{B}$ particles. The FM vacuum is unstable at the FM-PM transition with respect to $\mathscr{H}_{\mathrm{eff}}^{(2)}$ which transforms that vacuum state $\ldots \mathscr{B}\mathscr{B}\mathscr{B}\mathscr{B} \ldots$ into the set of $\ldots \mathscr{B} \ldots \mathscr{B}\mathscr{A}\mathscr{A}\mathscr{B} \ldots \mathscr{B} \ldots$ functions, that means $p = 2$. On the contrary, the $\langle 2 \rangle$ phase is described as the $\ldots \mathscr{A}\mathscr{A}\mathscr{A}\mathscr{A} \ldots$ vacuum. According to the definition when $\mathscr{A}$ (or DW) disappears, it creates a couple $\mathscr{B}\mathscr{B}$. Hence, the elementary excitation due to $\mathscr{H}_{\mathrm{eff}}^{(2)}$ can be represented as $\ldots \mathscr{A} \ldots \mathscr{A}\mathscr{B}\mathscr{B}\mathscr{B}\mathscr{B}\mathscr{A} \ldots \mathscr{A} \ldots$, which is irrelevant ($p = 4$).

A fictitious lattice as it has been introduced in [9] is better realized in the case of infinite chain with no periodic boundary conditions imposed. The fictitious lattice sites are enumerated as $\tilde{m} = m - \eta(m)$, where $\eta(m) = \sum_{i<n} n_i$ is the total number of fermions from the left of the m-th site of a real lattice. For fermions on the fictitious lattice we accept the notation $\tilde{c}_{\tilde{j}}$ ($\tilde{c}_{\tilde{m}}^\dagger$). $\mathscr{H}_{\mathrm{eff}}^{(1)}$ is formally unchanged:

$$\tilde{\mathscr{H}}_{\mathrm{eff}}^{(1)} = \sum_{\tilde{m}} \varepsilon \tilde{n}_{\tilde{m}} - \Gamma(\tilde{c}_{\tilde{m}}^\dagger \tilde{c}_{\tilde{m}+1} + \tilde{c}_{\tilde{m}+1}^\dagger \tilde{c}_{\tilde{m}}) \tag{22}$$

while $\mathscr{H}_{\mathrm{eff}}^{(2)}$ takes a form:

$$\tilde{\mathscr{H}}_{\mathrm{eff}}^{(2)} = -\gamma \sum_{\tilde{m}} (\tilde{c}_{\tilde{m}}^\dagger \tilde{c}_{\tilde{m}+1}^\dagger P_+(\tilde{m}+1) + \tilde{c}_{\tilde{m}+1} \tilde{c}_{\tilde{m}} P_-(\tilde{m}+1)) \tag{23}$$

where the operator $P_+(\tilde{m})(P_-(\tilde{m}))$ translates all the fermions from the right of $\tilde{m}$ by two sites to the right (left).

III. Exact diagonalization of finite systems

The starting point for our numerical investigation of the ground-state properties of the ANNNI-model (1) is the effective Hamiltonian $\mathscr{H}_{\mathrm{eff}}^{(1)}$ without creation/annihilation of domain walls (8), which we call the *free model* and the effective Hamiltonian $\mathscr{H}_{\mathrm{eff}}^{(1)} + \mathscr{H}_{\mathrm{eff}}^{(2)}$, which includes creation/annihilation of domain walls (19) and which we call the *complete model*. The Hilbert space for these models consists of all configurations of the original ANNNI-model, which obey the constraint discussed in the last section. This constraint reduces the dimension of the Hilbert space considerably so that much larger system sizes can be diagonalized (even if one uses the translational and spin flip symmetry of the original ANNNI Hamiltonian to block diagonalize it first).

A. Methodology

We reformulate the constraint in such a way that it becomes suitable for a numerical implementation. The domain walls can be identified with particles being able to hop to the left or right provided the constraint will not be violated by this move (moreover at most one particle can occupy a single site in the dual lattice). Since a domain wall at bond j comes always with bond $j+1$ free of domain walls we call this combined object an $\mathscr{A}$-particle situated at bond j. If no domain wall is at bond j we call it a $\mathscr{B}$-particle provided no other domain wall occurs at bond $j-1$. In an obvious notation the following particle configuration, domain wall (i.e. τ-) configuration and spin configuration (in the σ_z-representation) correspond to each other

$$|\mathscr{A}\mathscr{A}\mathscr{B}\mathscr{B}\mathscr{A} \cdots\rangle = |10100010 \cdots\rangle = \begin{cases} |\uparrow\downarrow\downarrow\uparrow\uparrow\uparrow\uparrow\downarrow \cdots\rangle \\ |\downarrow\uparrow\uparrow\downarrow\downarrow\downarrow\uparrow \cdots\rangle \end{cases}. \tag{24}$$

Moving a domain wall from bond i to $i \pm 1$ means moving an $\mathscr{A}$-particle from site i to $i \pm 1$, which is only possible, if at site $i \pm 1$ is a $\mathscr{B}$-particle.

$$\begin{aligned} \tau_1^+ \tau_2^- |\mathscr{B}\mathscr{A} \cdots \rangle &= |\mathscr{A}\mathscr{B} \cdots \rangle \\ \tau_1^- \tau_2^+ |\mathscr{A}\mathscr{B} \cdots \rangle &= |\mathscr{B}\mathscr{A} \cdots \rangle \end{aligned} \tag{25}$$

Thus in the particle representation the above mentioned constraint is already contained. Analogous remarks hold for the creation/annihilation of domain walls described by $\mathscr{H}_{\text{eff}}^{(2)}$: in the particle formulation that means that $\mathscr{A}$-particles can be created in pairs in place of four consecutive $\mathscr{B}$-particles. For instance

$$\begin{aligned} \tau_1^+ \tau_3^+ |\mathscr{B}\mathscr{B}\mathscr{B}\mathscr{B} \cdots \rangle &= |\mathscr{A}\mathscr{A} \cdots \rangle \\ \tau_1^- \tau_3^- |\mathscr{A}\mathscr{A} \cdots \rangle &= |\mathscr{B}\mathscr{B}\mathscr{B}\mathscr{B} \cdots \rangle \end{aligned} \tag{26}$$

Because of the periodic boundary conditions we have to discriminate between the cases with and without a domain wall at bond L. We denote the first group of states with a prime, for instance (in the case of L = 8):

$$|\mathscr{A}\mathscr{B}\mathscr{B}\mathscr{A}\mathscr{A}\rangle' = |01000101\rangle \tag{27}$$

(note that in this notation the rightmost particle is always an $\mathscr{A}$-particle), whereas those without prime denote states without domain wall between L and 1, e.g.:

$$|\mathscr{A}\mathscr{B}\mathscr{B}\mathscr{A}\mathscr{A}\rangle = |10001010\rangle \tag{28}$$

This state is simply a circular left shift of the primed state in (27), in fact for each primed state there is a unique unprimed state that can be obtained from the former via a circular left shift. However, there are of course more primed states than unprimed ones.

Thus we consider different primed and unprimed subspaces characterized by the number of $\mathscr{A}$-particles (i.e. number of domain walls), which is conserved under the action of $\mathscr{H}_{\text{eff}}^{(1)}$ (note, however, that the latter mixes states of the primed and unprimed subspaces by moving domain walls to or from the bond L. The dimension of these subspaces is simply given by the number of different possibilities to distribute n_A and $n_A - 1$ particles on $L - n_A$ and $L - n_A - 1$ sites, respectively.

$$\begin{aligned} \dim_{n_A} &= \binom{L - n_A}{n_A}, \\ \dim'_{n_A} &= \binom{L - n_A - 1}{n_A - 1}. \end{aligned} \tag{29}$$

The dimension of the whole Hilbert space we are considering is

$$\dim_{\mathscr{H}_{\text{eff}}} = 1 + \sum_{n_A = 1}^{L/2} \left\{ \binom{L - n_A}{n_A} + \binom{L - n_A - 1}{n_A - 1} \right\} \tag{30}$$

which is a much smaller number than the dimension of the original Hilbert space, which is 2^L.

From Table 1 it becomes obvious that the storage requirements for diagonalizing the effective Hamiltonian is significantly smaller. This is still the case if one uses all symmetries of the original ANNNI Hamiltonian to block-diagonalize it first (by which can reduce the storage requirement by roughly a factor $1/L$). Note that in the FP-phase it is not a priori clear in which wave number sector of the original Hilbert state the ground state is situated. Hence all of them have to be considered, as has been done in [15] for lattice site up to $L = 16$. We were able to diagonalize easily L = 32 systems on workstations with a reasonable RAM without reading or writing to the hard disk.

Table 1. Dimensionality of the reduced Hilbert space of our effective Hamiltonians (second column) and the dimensionality of the original Hilbert space (third column)

L	$\dim_H$	2^L	$\dim_H/2^L$
8	23	256	8.984375e-02
12	162	4096	3.955078e-02
16	1103	65536	1.683044e-02
20	7563	1048576	7.212639e-03
24	51842	16777216	3.090024e-03
28	355323	268435456	1.323681e-03
32	2435423	4294967296	5.670411e-04

In order to enumerate the states within the subspaces efficiently we recur to a scheme that is frequently used in the context of quantum spin chains confined to subspaces ith constant magnetization [14]. Let us fix L to be a multiple of 4 (so that the periodic boundary conditions are fully compatible with the ground state in the anti-phase $\langle 2 \rangle$). Let $\psi_{n_A}(n)$ be an unprimed state with n_A $\mathscr{A}$-particles:

$$\psi_{n_A}(n) = |\mathscr{A}(p_1 \cdots \mathscr{A}(p_{n_A})\rangle = |\underbrace{\mathscr{B} \ldots \mathscr{B}}_{p_1 - 1} \mathscr{A} \underbrace{\mathscr{B} \ldots \mathscr{B}}_{p_2 - p_1 - 1} \mathscr{A} \ldots \ldots \rangle \tag{31}$$

where $p_i \in \{1, \ldots, L - n_A\}$ denotes the position of the i-th $\mathscr{A}$-particle (counted from the left). Then the following definition yields a one-to-one correspondence between the possible configurations and a number $n \in \{0, \ldots, \dim_{n_A} - 1\}$:

$$n = \sum_{i=1}^{n_A} \binom{p_i - 1}{\mathrm{i}} \quad \text{with} \quad \binom{i - 1}{i} = 0. \tag{32}$$

The same definition is used for primed and unprimed states, which we denote by $\psi'_{n_A}(n)$ and $\psi'_{n_A}(n)$, respectively. The Lanczos routine we use to calculate the ground state and first excited state generates the Hamiltonian each time it is needed, for this reason we need to know how the various hopping, creation and annihilation operators act upon the basis states we have chosen. This can either be done by a hashing technique, which is used frequently for arbitrary quantum spin chains, or by explicitly calculating the number of the transformed state if possible. Fortunately in our case the latter is straightforward, and in Appendix D we list all relevant formulas that we need to generate the non-zero matrix elements for $\mathscr{H}_{\text{eff}}^{(1)}$ and $\mathscr{H}_{\text{eff}}^{(2)}$.

With the help of nowadays standard Lanczos routines we calculated the ground state and the first excited state of systems of size up to L = 32. The effective Hamiltonians we derived are expected to be good approximations to the original ANNNI model for small values of Γ/J. We confined ourselves to the values $\Gamma/J = 0.05$, 0.1, 0.2 and 0.5, where we calculated all physical quantities of interest for

κ-values in intervals of $5{\cdot}10^{-4}$. We performed extensive checks of our code by comparing our numerical estimates for the ground state energy and the gap with the exactly known values for the free model (8). We also compared our results obtained for $\mathscr{H}^{(1)}_{\text{eff}} + \mathscr{H}^{(2)}_{\text{eff}}$ at small values of Γ/J with those for the original ANNNI model and found no significant deviations.

B. Results

In order to check the quality of the free fermion description we first calculated the ground states of the original ANNNI model (1)–(2) for a modest system size (up to $L = 20$). The "classical" energy of a state

$$E_{\text{class}} = \langle \psi | H_{\text{cl}} | \psi \rangle \tag{33}$$

which is $E_{\text{class}} = -\mathscr{J}(\sum_i S_i S_{i+1} - \kappa \sum_i S_i S_{i+2})$ for an eigenstate of the σ_i^z operators contains the information on the average number of domain walls (or $\mathscr{A}$-particles) in the state ψ, if this last does allow neither $\ldots\uparrow\downarrow\uparrow\ldots$, nor $\ldots\downarrow\uparrow\downarrow\ldots$ to appear. With such a constraint imposed on a state with exactly $n_A \in \{0, 2, 4, \ldots, L/2\}$ domain walls, each of them costing an energy $\varepsilon = -(4\kappa - 2)\mathscr{J}$ with respect to the FM state, we have

$$E_{\text{class}}/\mathscr{J} + (1 - \kappa)L = n_A \cdot (4\kappa - 2) \tag{34}$$

Thus the comparison of the l.h.s. which we call *DE*, with the set of straight lines provides a measure of the average number of $\mathscr{A}$-particles plus an indication of the appropriateness of the free fermion concept in this context. In Fig. 2 we show the result for various values of Γ and we see that the smaller Γ the better the agreement of various parts of the *DE*-curves. Furthermore, for increasing Γ the ground state is more a superposition of various particle eigenstates *in the vicinity of the FM-PM transition.*

Now we turn our attention to the effective Hamiltonians. The average number of domain walls, simply given by $\langle n_A \rangle = \langle \psi | \sum_i \tau_i^+ \tau_i^- | \psi \rangle$ is calculated for ψ's of the ground state and of the first excited state of the complete model (8) + (19). For Γ not too large one observes well defined regions with constant value for n_{A} in the ground state and the first excited state. See Fig. 3 for an example. The number of $\mathscr{A}$-particles increases monotonically (in steps of 2) for increasing κ. The points where the particle number jumps are of special interest. The particle number of the first excited state $\langle n_A \rangle_1$ jumps first abruptly (approaching the transition points from either side) and then it changes roles with the ground state. As a consequence the gap (i.e. the energy difference between ground state and first excited state) gets very small here.

Note that in the FM-phase the gap does *not* vanish exponentially with system size for the effective Hamiltonians, because in the particle representation the two degenerated states with all spins up or all spins down are represented as *one* state. Therefore the gap closes in the infinite system only *at* the FM-PM transition. On the other hand the gap stays zero (or exponentially small for finite sizes) throughout the $\langle 2 \rangle$ phase also for the effective Hamiltonians: The 4-fold degeneracy there is only reduced by a factor two via the elimination of the spin-flip

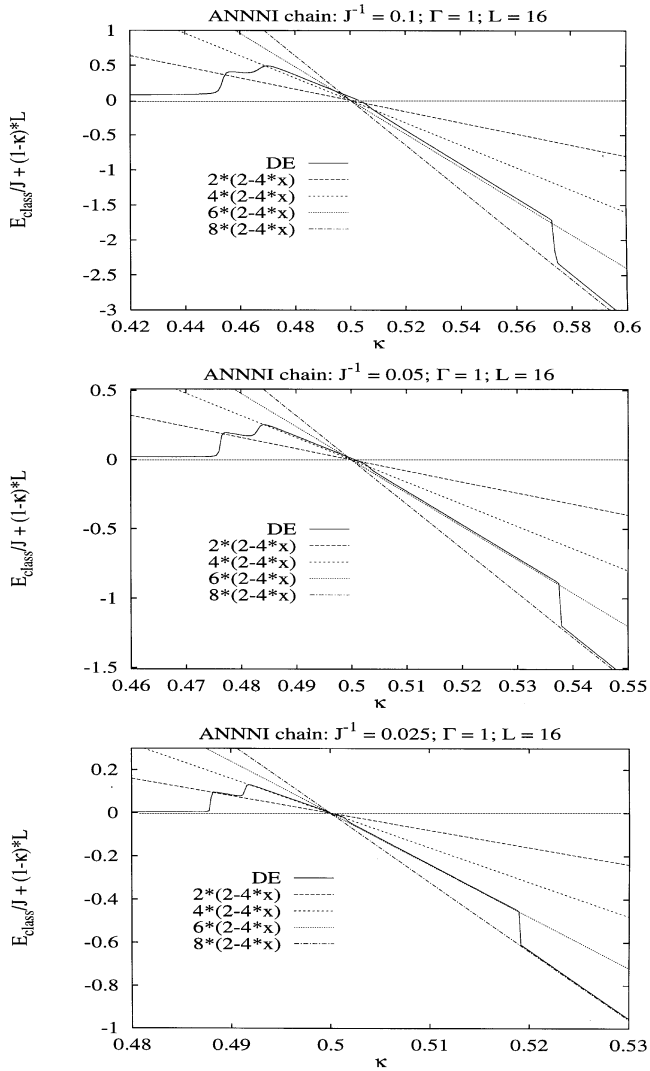

Fig. 2. Results of exact diagonalization of the original ANNNI model (1)–(2) for $L = 16$ and various values of Γ/J: Expectation value of the quantity $E_{\text{class}}/J + (1 - \kappa)\, L$ defined in the text

symmetry and a degeneracy between corresponding primed and unprimed states is left.

As a significant difference of the complete model with respect to the free model we note that at the special κ-values, where the particle number changes and which can be calculated exactly via the formula (13), the gap of the free model (8) closes completely, i.e. $\Delta E^{\text{free}}_{n_A \to n_A \pm 2} = 0$. In the complete model the gap-value on the boundary, say, $n_A \to n_A + 2$, can be easily estimated if we confine our consideration with these two competing states only, that results in

$$\Delta E_{n_A \to n_A + 2} = 2 \langle \psi_{n_A + 2} | \mathscr{H}^{(2)}_{\text{eff}} | \psi_{n_A} \rangle \tag{35}$$

These special gap-values increase with Γ because of the Γ-dependent $\mathscr{H}^{(2)}_{\text{eff}}$. In particular more pronounced is the gap increasing for the lower κ-values. In this range the boundary $n_A \to n_A + 2$ cannot be considered as well isolated from other "neighboring" states, *i.e.*, $n_A - 2$, $n_A + 4$, etc. This observation will turn out as a hint for the existence of the PM-FP transition. For higher values of Γ/J

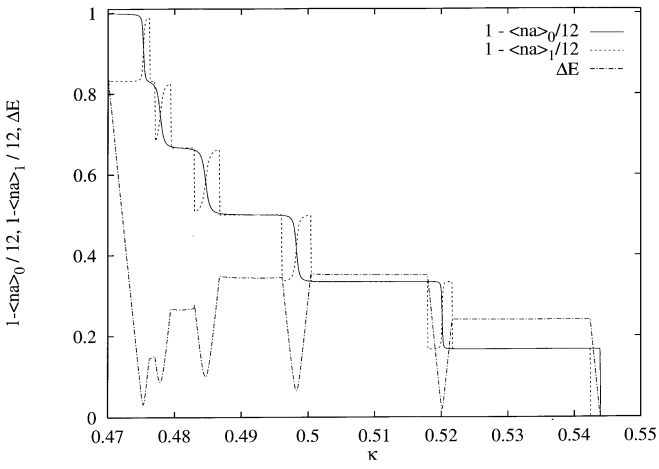

Fig. 3. Results of exact diagonalization of the complete model (8) + (19). Shown are the results for the expectation value of the particle number in the ground state and the first excited state together with the gap ΔE. It is $L = 24$ and $\Gamma/J = 1/20$

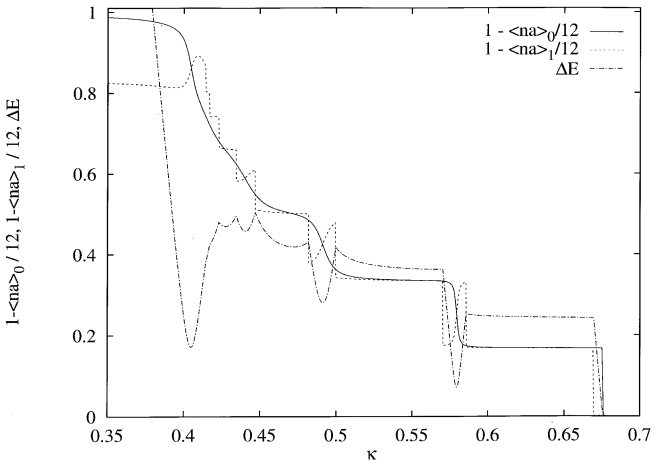

Fig. 4. The same as in Fig. 3 but with $\Gamma/J = 1/5$

the resulting picture is therefore slightly different: the transitions smear out and $\langle n_A \rangle(\kappa)$ and ΔE become smoother as can be seen in Fig. 4.

Let us interpret this picture *cum grano salis*: One might tentatively locate the FM-PM transition (for $\Gamma/J = 1/5$) roughly at $\kappa \approx 0.41$, where the gap should approach zero like $\Delta E \sim 1/L$ (since the transition is expected to be in the Ising universality class, where $\nu = z = 1$). Between $\kappa = 0.41$ and let us say $\kappa \approx 0.48$ the average particle number increases from zero to 8 (for $L = 24$), but the individual transitions observable in Fig. 3 *melt* together to form a rugged plateau. Only when n_A gets larger than some value (whose significance we will clarify later) the gaps at the individual transitions try to close again. With increasing system size these gaps (for κ larger than roughly 0.48) melt together, too, but in the limit $L \to \infty$ they will form a curve $\Delta(\kappa) = 0$ in this region, which is simply the gapless floating phase with a *quasi*-long range, i.e., algebraically decaying spin correlations.

It is obvious that in order to observe this scenario in its pure form one has to go to enormous system sizes, which is not feasible yet. Nevertheless we can clearly demonstrate the qualitative difference between the PM phase and the FP phase by explicitly studying the spin correlations in both regions of the phase diagram for intermediate system sizes.

The spin correlation function is defined via

$$C(r) = \langle \psi | \sigma_i^z \sigma_{i+r}^z | \psi \rangle$$

$$= \sum_{n_A=0}^{L/2} \sum_{n=0}^{\dim_{n_A}} \psi_{n_A}^2(n) \cdot \frac{1}{L} \sum_{i=1}^{L} S_i[\psi_{n_A}(n)]$$

$$S_{i+r}[\psi_{n_A}(n)] + \text{primed states}. \tag{36}$$

Here $\underline{S}[\psi_{n_A}(n)]$ ($\underline{S} = S_1, \ldots, S_L$) means the spin configuration that is equivalent to the state number n with n_A particles (since there are always two of them we choose the one with the first spin up $S_1 = +1$). Of course we have to initialize such a mapping in our program once, afterwards this table can be used whenever correlations have to be calculated.

First we take a look at the structure function since this directly relates to the particle number n_A discussed above. We define it as follows: via

$$f_q(\kappa) = \frac{1}{L^2} \sum_{i,j} \cos(q(i-j)) \langle \psi | \sigma_i^z \sigma_j^z | \psi \rangle \tag{37}$$

for $q = n/L$ ($n = 0, 1, \ldots, L-1$) so that

$$C(r) = \sum_q \cos(qr) f_q \tag{38}$$

In Fig. 5 we show the result for $f_q(\kappa)$ for $\Gamma/J = 1/20$ in comparative plots for the free and the complete model. For fixed wave number q the structure function $f_q(\kappa)$ is simply a step function for the free model, the plateaus located at the κ-intervals with constant particle number n_A. For fixed κ the wave number $q_{\max}$ with the maximum amplitude $f_{q_{\max}}(\kappa) > f_q(\kappa)$ for $q \neq q_{\max}$ is related to the particle number n_A via

$$q_{\max} = n_A/2L \tag{39}$$

(note that n_A is a good quantum number in the free model). For small Γ/J we observe that the steps get rounded, but nothing dramatic (for these system sizes) happens. If we increase Γ/J, as is done in Fig. 6, the neighboring plateaus begin to mix (to melt, see above). They also shift their location to larger values of κ. However, these changes seem to become less significant as soon as $q_{\max}$ is larger than 1/4. Actually, as stated in the last section in Eq. (18), the theoretical estimate for this relevance-threshold is $q = 0.292 > 1/4$ for the free model and approximately this value for the complete model for small Γ/J.

This statement finds its strongest support by looking at the spin correlation function (36), shown in Fig. 7 and 8 for $L = 32$, directly. For the free model of finite size L with periodic boundary conditions one would according to (17) expect that

$$G(r) = a \cos(r\pi q_{\max}) \cdot \{r^{-\rho} - (L-r)^{-\rho}\} \quad \text{with}$$

$$\rho = \frac{1}{2}(1 - q_{\max})^2, \tag{40}$$

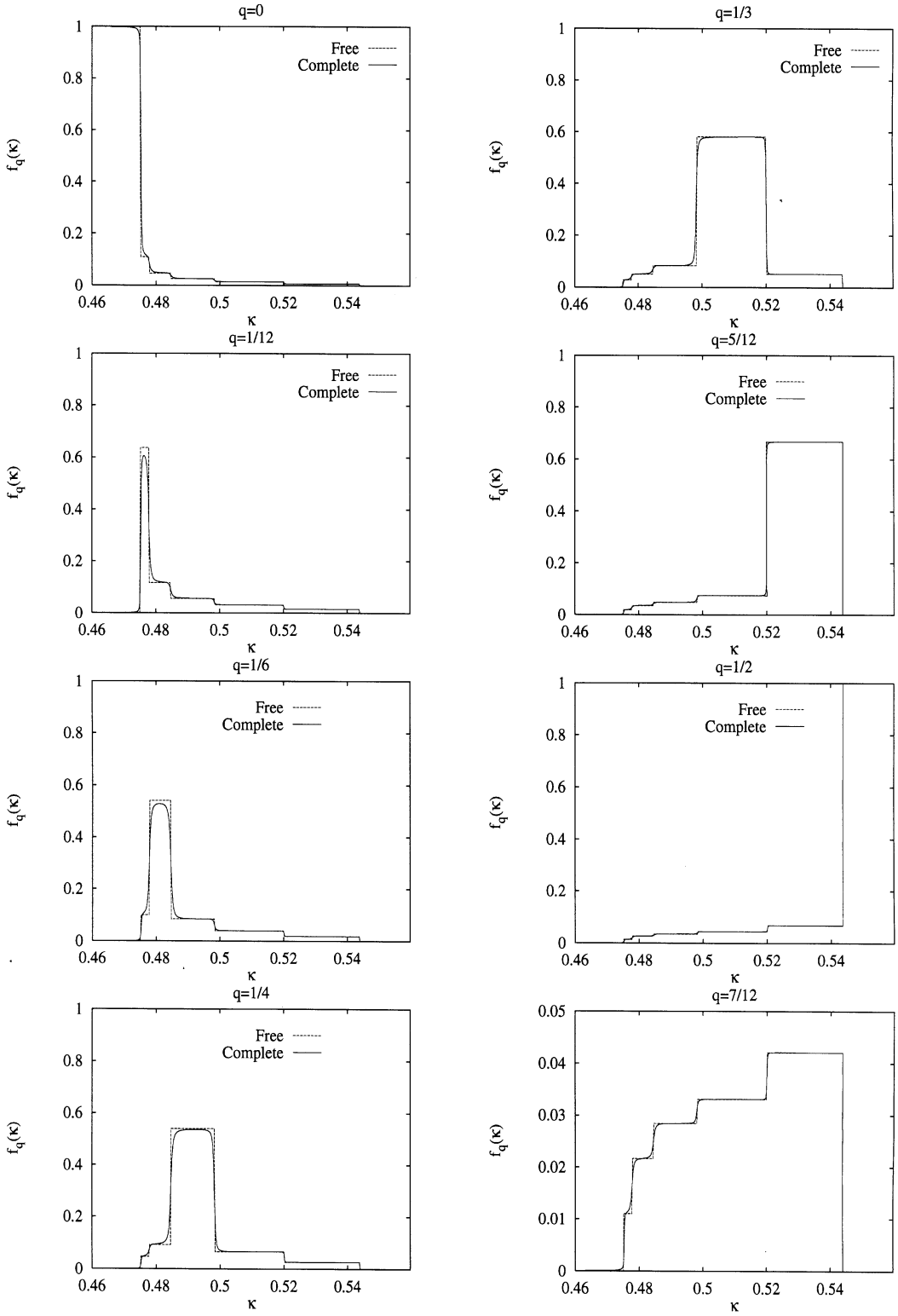

Fig. 5. Comparison of the structure function $f_q(\kappa)$, Eq. (37), for the free and the complete model. It is L = 24 and $\Gamma/J = 1/20$. Note the different scale on the y-axis in the plot for $q = 7/12$

where a is a fit parameter and $q_{\max}$ has to be determined from the structure function. In order to resolve the correlations over as large as possible distances we took here the largest possible system sizes. For $L = 32$, however, we had to confine ourselves to a smaller number of parameter values. In the case $\Gamma/J = 1/20$, in which the differences between the complete and the free model are not too large, we took simply the middle of the plateaus of the structure

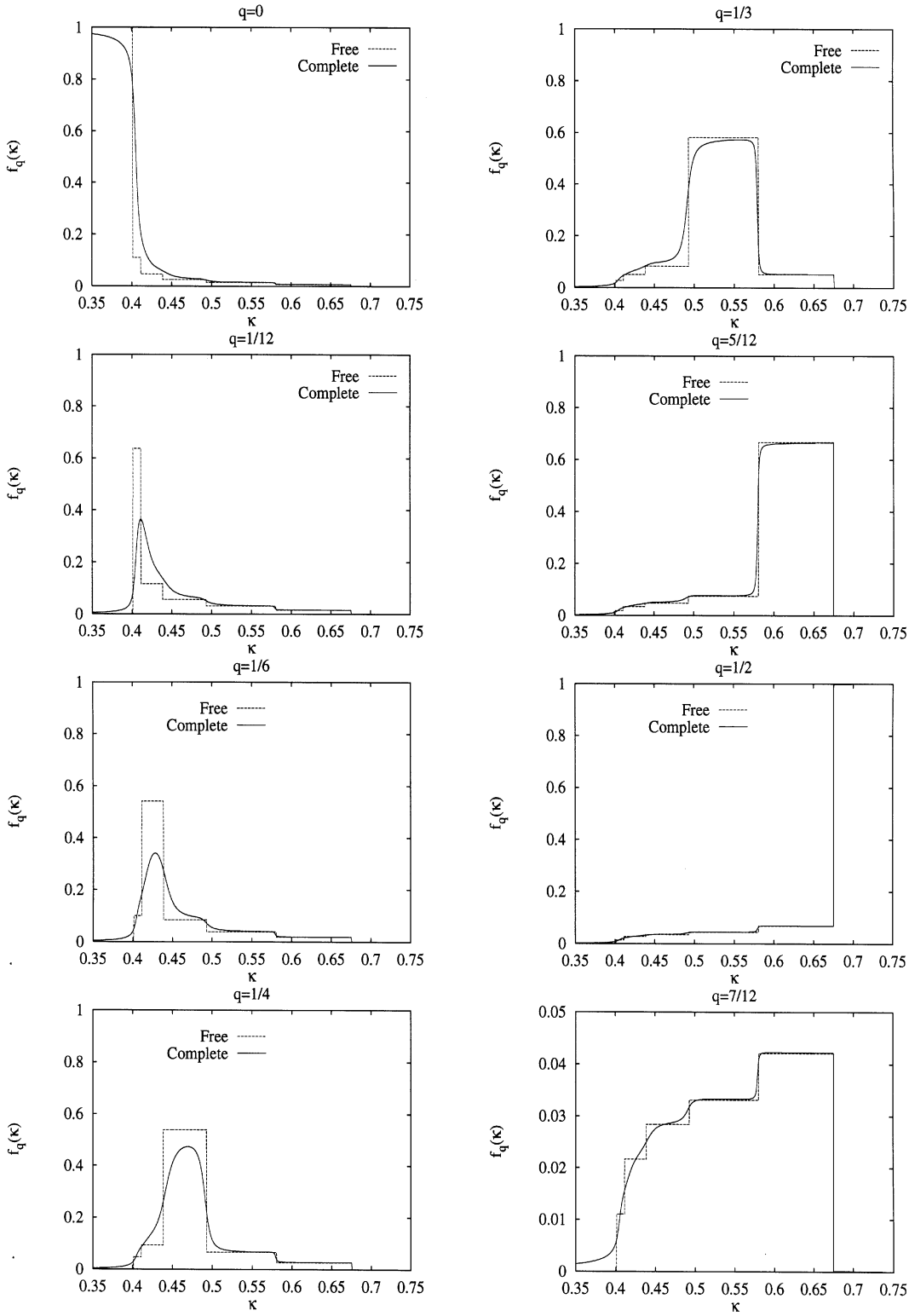

Fig. 6. The same as in Fig. 5 but with $\Gamma/J = 1/5$

function, wehreas for Γ/J we took the location of the maxima of $f_q(\kappa)$ shown in Fig. 9.

What is shown in Fig. 7 and 8 is a comparative plot of $C(r)$ and $G(r)$ with $a = \sqrt{\Sigma_r C^2(r)/\Sigma_r \tilde{G}^2(r)}$, $\tilde{G}(r) = G(r)/a$. We observe that for $q_{\max} > 1/4$ the free model correlation function $G(r)$ fits $C(r)$ in an excellent way. For $q_{\max} \leq 1/4$, however, one recognizes significant differences between $G(r)$ and $C(r)$, most dramatic for the smallest wave

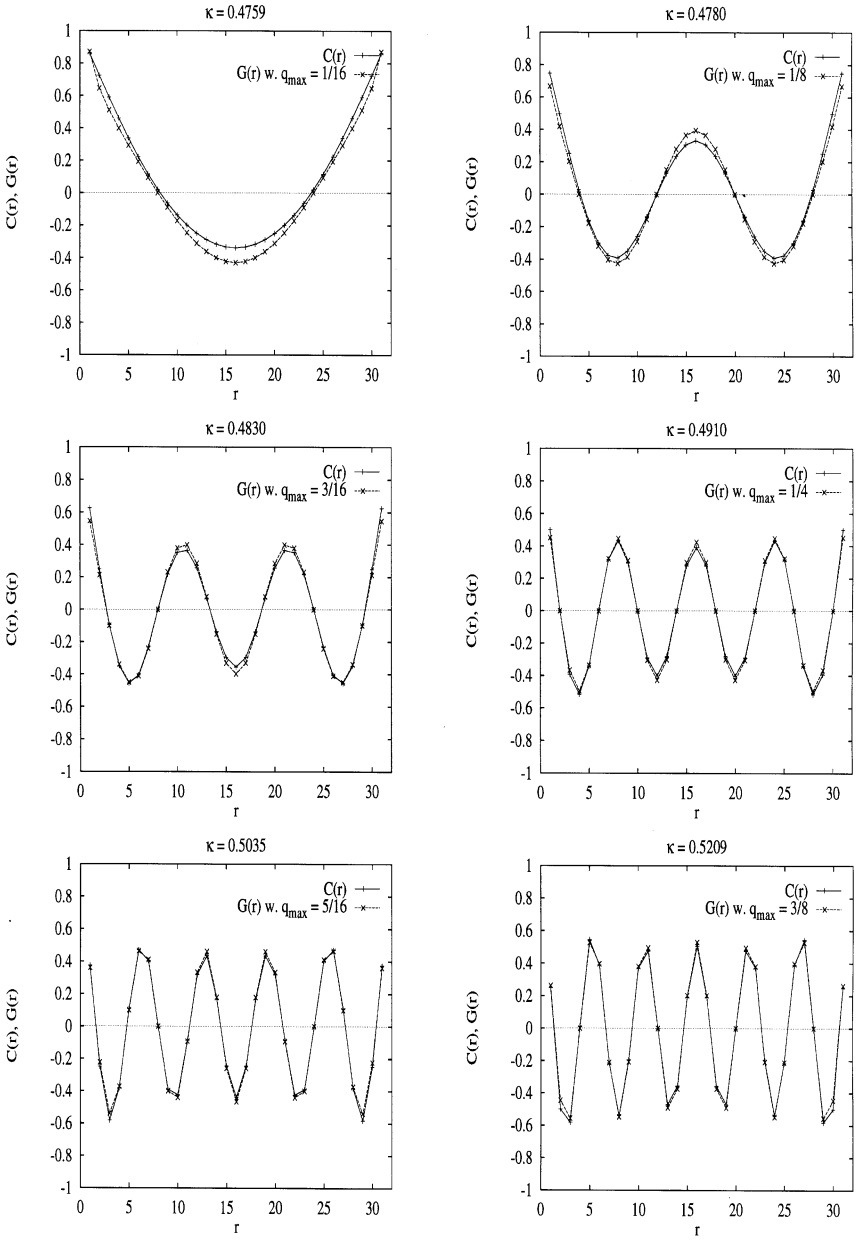

Fig. 7. Comparison of the correlation function C(r), Eq. (36), of the complete model with $G(r)$ given in (40). It is L = 32 and $\Gamma/J = 1/20$

numbers, which mean closest to the FM-PM transition of the complete model. The $q_{\max} = 1/12$ and $q_{\max} = 1/6$ curves for $\Gamma/J = 154$ definitely decay faster than algebraic. We obtained an excellent fit (shown in Fig. 10 for the $q_{\max} = 1/16$ curve by a superposition of an exponentially damped $q = 0$ and $q = 1/16$ oscillation:

$$C_{\kappa = 0.4085;\Gamma/J = 5}(r) = (1 - a + a\cos(r\pi/16)) \cdot (e^{-r/\xi} + e^{-(32-r)/\xi}) \tag{41}$$

with $a = 0.21$ and $\xi = 3.6$. For us this is ample evidence that for fixed Γ/J one enters first a paramegentic phase with exponentially decaying correlations by increasing κ from rthe FM-phase. Only when $q_{\max}$ gets larger then the above mentioned value, one enters the FP-phase, which for the free model extends over the whole region between the $\langle 2 \rangle$ and FM phses.

IV. Summary

Below we summarize a few important points of this work.

- Instead of the original 1d ANNNI model in a transverse field we consider a reduced model which we show to be a very reasonable modification when the competition parameter $|\kappa - 1/2|$ as well as the quantum parameter $\Gamma/\mathscr{J}$ are small.
- The effective Hamiltonian $\mathscr{H}^{(1)}_{\text{eff}} + \mathscr{H}^{(2)}_{\text{eff}}$ is most easily visualized with the $\mathscr{A} - \mathscr{B}$ particle representation. The latter has been adapted to the periodical boundary conditions and efficiently used in numerical calculations.
- Analytical calculations here were done not for rediscovering after [9] the essential physics, accompanying the scheme of phase transitions FM-PM-FP-$\langle 2 \rangle$ in infinitely long chains. Most analytical results are derived for further applications in a numerical scheme.

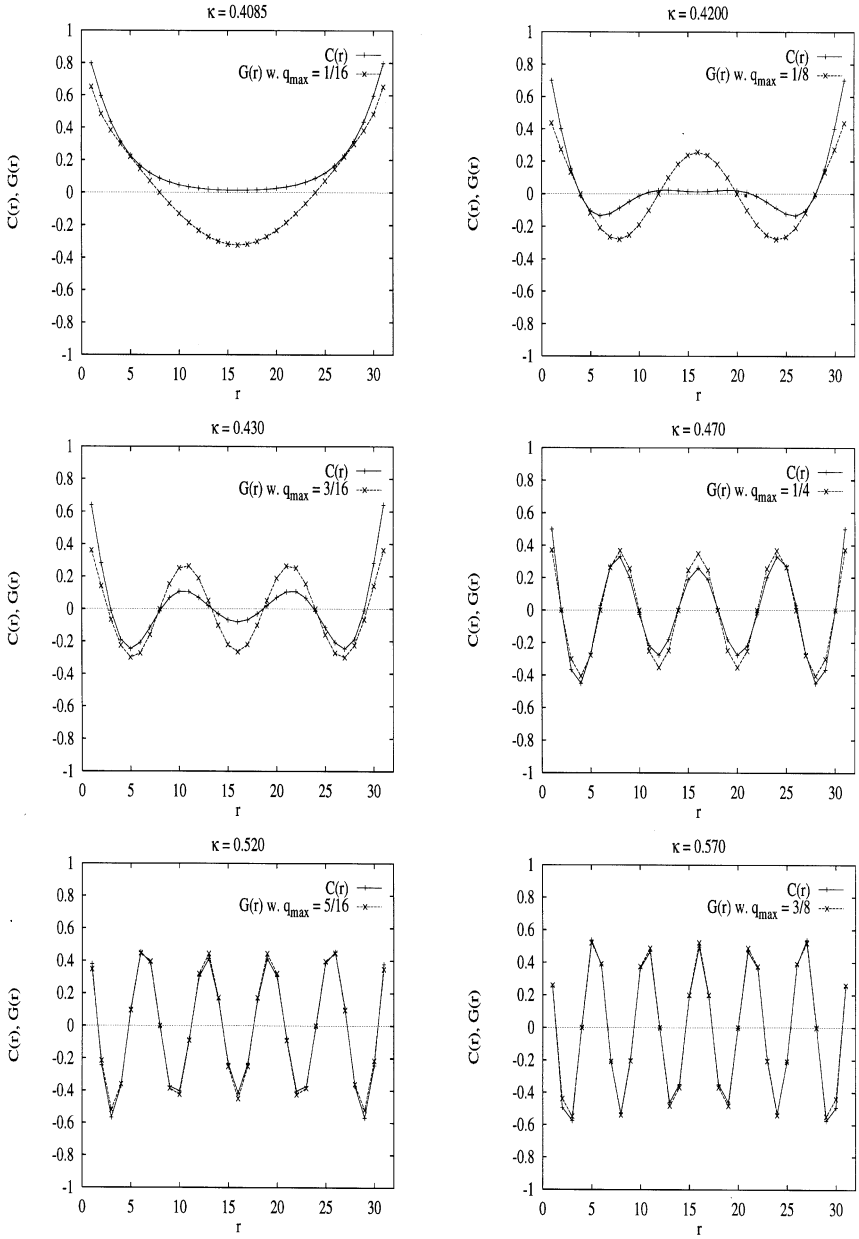

Fig. 8. The same as in Fig. 7 but with $\Gamma/J = 1/5$

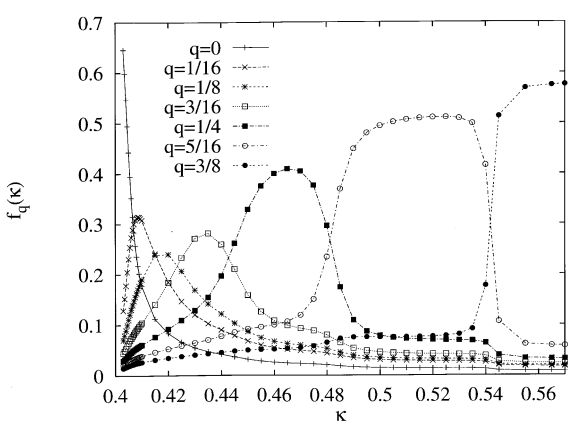

Fig. 9. Structure function $f_q(\kappa)$, Eq. (37), for the complete model in the case L = 32 and $\Gamma/J = 1/5$

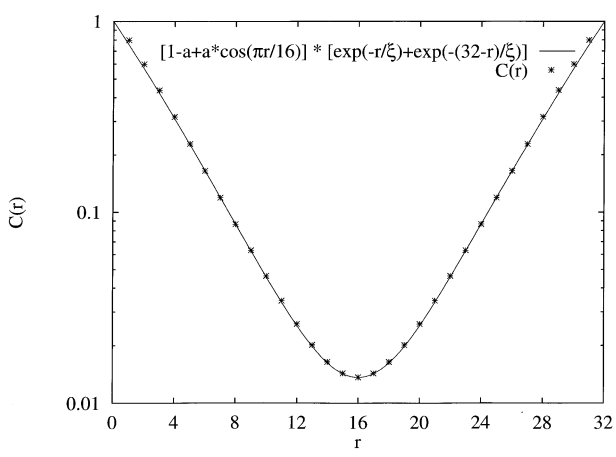

Fig. 10. Fit of (41) to the correlation function $C(r)$ for $\kappa = 0.4085$, the maximum of the $f_{q=1/12}$ curve shown in Fig. 9. It is L = 32 and $\Gamma/J = 1/5$. The fit parameters are $a = 0.21$, $\xi = 3.6$

- The exact numerical diagonalization technique (Lanczos algorithm) was used on the restricted basis states, all of them have been enumerated, as well as all the non-zero matrix elements generated by Hamiltonian of the complete model were stored. Along this line we perform calculations for systems of size up to L = 32 with standard work-stations.
- The set of Figs. 5–10 convincingly illustrates a different origin of the critical behavior at larger and smaller κ's. Most likely, the PM-FP transition takes place close to or even at a modulation q given by the theory of the standard Kosterlitz-Thouless-like transition.

This work has been performed within the Sonderforschungsbereich (SFB) 341 Köln-Aachen-Jülich. G.U. thanks the Institut f. Theoretische Physik of the University of Köln for its kind hospitality and H.R. thanks S. Dasgupta for numerous fruitful discussions and numerical experiments on the ANNNI-model.

Appendix A

We treat τ_j^z as a domain wall operator, defined on the lattice site j of the dual lattice. It takes two values, ± 1: $+1$ (-1) signals of absence (presence) of a domain wall. Mathematically, this can be expressed by

$$\tau_j^z = \sigma_{j-1/2}^z \sigma_{j+1/2}^z. \tag{A.1}$$

Because of the periodic boundary conditions we also define

$$\tau_1^z = \sigma_{1/2}^z \sigma_{3/2}^z \quad \text{and} \quad \tau_L^z = \sigma_{1/2}^z \sigma_{L-1/2}^z. \tag{A.2}$$

Also evidently, that

$$\tau_j^z \tau_{j+1}^z = \sigma_{j-1/2}^z \sigma_{j+3/2}^z. \tag{A.3}$$

For x-components we accept the following definitions:

$$\sigma_{j+1/2}^x = \tau_j^x \tau_{j+1}^x \tag{A.4}$$

and

$$\sigma_{1/2}^x = \tau_1^x \tau_L^x \quad \text{and} \quad \sigma_{L-1/2}^x = \tau_{L-1}^x \tau_L^x. \tag{A.5}$$

With using (A.1), (A.3) and (A.4) we can easily obtain the form of (6) from (1).

This transformation set allows to calculate the correlation functions in terms of τ's, for example:

$$\langle \sigma_{r_1-1/2}^z \sigma_{r_2+1/2}^z \rangle = \left\langle \prod_{j=r_1}^{r_2} \tau_j^z \right\rangle \tag{A.6}$$

Appendix B

In Eq. (10) m's are supposed to be arranged in order, satisfying the following constraints: $m_1 < m_2 - 1$, $m_2 < m_3 - 1, \ \dots, m_{k-1} < m_k - 1, \ m_k < m_1 + L - 1$. We transfer these constraints on the amplitudes f:

$$f(\dots, m, m+1 \dots) = 0 \tag{B.1}$$

$$f(1, \dots, L) = 0. \tag{B.2}$$

In spite of the irregular $1 \leftrightarrow L$ hopping term in (9) the eigen amplitudes f satisfy the regular equations:

$$(E - k\varepsilon) f(m_1, m_2, \dots, m_k) = -\Gamma \sum_{a = \pm 1} (f(m_1 + a, m_2, \dots, m_k) f(m_1, m_2 + a, \dots, m_k) + \dots + f(m_1, m_2, \dots, m_k + a)). \tag{B.3}$$

Using a Bethe substitution for f's (see (8)) we obtain

$$E = k\varepsilon - 2\Gamma \sum_{j=1}^{k} \cos q_j. \tag{B.4}$$

Equations (B.1) and (B.2) yield

$$\xi_{\dots ij \dots} e^{iq_j} + \xi_{\dots ji \dots} e^{iq_i} = 0 \tag{B.5}$$

and

$$\xi_{i \dots j} e^{i(q_i + Lq_j)} + \xi_{j \dots i} e^{i(q_j + Lq_i)} = 0, \tag{B.6}$$

respectively. In turn, from (B.5) and (B.6) one can arrive to

$$q_i - q_j = \frac{2\pi}{L - k} n_{ij} \tag{B.7}$$

where n_{ij} are integer numbers. Additional equations imposed on q's may be obtained from (B.3) at $m = 1$. Formally, it is equivalent to $f(0, m_2, \dots, m_k) = f(m_2, \dots, m_k, L)$, that is

$$\xi_{ijs \dots t} = \xi_{js \dots ti} e^{iLq_i} \tag{B.8}$$

which after a simple algebra results in

$$q_i = \frac{\pi n_i^{\text{odd}}}{L - k} - \frac{1}{L - k} \sum_{j=1}^{k} q_j, \tag{B.9}$$

$[n^{\text{odd}}\}$, the set of odd integer numbers.

The content of this Appendix may be summarized in this last (B.9) and the form of the the eigenfunctions (12).

Appendix C

For the ground state of k DW's the set $\{n^{\text{odd}}\}$ in (B.9) counts all the equidistant odd numbers from $-k+1$ to $k-1$. Let us take away one number from that set, say, $n_-^{\text{odd}} = 2v_- - 1$, with $-k/2 + 1 < v_- < k/2 - 1$, and add another number $n_+^{\text{odd}} = 2v_+ - 1$, with $v_+ > k/2$. With this definition $\sum n_i^{\text{odd}} = 2(v_+ - v_-)$ and after summation in both parts of (B.9) we get

$$Q = \sum_i q_i = \frac{2\pi(v_+ - v_-)}{L} \tag{C.1}$$

The wavevectors in (B.9) are now determined and the energy of such an excitation counted from the ground

state energy takes a form:

$$\Delta E(Q) = -2\sum_i \cos q_i - E_{\rm gs}$$

$$= -2\sum_{v=-k/2+1}^{k/2} \cos\frac{(2v-1)\pi - Q}{L-k}$$

$$-2\cos\frac{(2v_+ - 1)\pi - Q}{L-k} + 2\cos\frac{(2v_- - 1)\pi - Q}{L-k}$$

$$+2\sum_{v=-k/2+1}^{k/2} \cos\frac{\pi(2v-1)}{L-k}$$

$$= 2\left(1-\cos\frac{Q}{L-k}\right)\sin\frac{\pi k}{L-k}\Big/\sin\frac{\pi}{L-k}$$

$$-2\sin\frac{Q}{L-k}\left[\sin\frac{\pi(2v_+-1)}{L-k} - \sin\frac{\pi(2v_- - 1)}{L-k}\right]$$

$$-2\cos\frac{Q}{L-k}\left[\cos\frac{\pi(2v_+-1)}{L-k} - \cos\frac{\pi(2v_- - 1)}{L-k}\right] \quad \text{(C.2)}$$

Using (C.2) we can analyze the lower lying excitations

1. $n_-^{\rm odd} = k-1$, $n_+^{\rm odd} = k+1 \Rightarrow Q = 2\pi/L$.

The excitation energy with a vanishing momentum transfer Q *in the* $L\to\infty$ limit reads in the leading order in $1/L$ (this contribution comes from the last term of the r.h.s. of (*C*.2)):

$$\Delta E(Q) \approx \frac{4\pi}{L-k}\sin\frac{\pi k}{L-k} = 2\Delta q \sin\frac{\pi k}{L-k} \quad \text{(C.3)}$$

where Δq is a q spacing (cf (B.7))

2. $n_-^{\rm odd} = -k+1$, $n_+^{\rm odd} = k+1 \Rightarrow Q = 2\pi k/L$.

All the terms in the r.h.s. of (B.7) contribute in the leading order in $1/L$. This excitation occurs at the energy

$$\Delta E(Q) \approx 2\Delta q\left(1-\frac{k}{L}\right)^2 \sin\frac{\pi k}{L-k} \quad \text{(C.4)}$$

which *differs* from (C.3).

3. For not a special value of Q a leading contribution, $O(1)$, comes from the last term of the r.h.s. of (C.2)). To leading order it can be written as:

$$\Delta E(Q) = 4\sin x \sin(x + 2\pi v_-/(L-k)), \quad x = \frac{QL}{2(L-k)}. \quad \text{(C.5)}$$

We used (C.1) to obtain the form of (C.5). Then in order to select the lowest energy values at fixed Q we consider following inequalities:

- $x < k_F = \pi k/(L-k)$. The possible range of v_-'s becomes $LQ/(2\pi) - k/2 < v_- < k/2$. The minimum of (C.5) is reached at the lower limit, that results in $\Delta E(Q) = 4\sin x \sin(k_F - x)$
- $k_{\rm F} < x < \pi - k_F$. Now a possible range of v_-'*s is* $-k/2 < v_- < k/2$. Two extreme possibilities should be checked, one arrives to the form $\Delta E(Q) = 4\sin x \sin(x - k_F)$, another results in $\Delta E(Q) = 4\sin x \sin(k_{\rm F} + x)$. The former realizes the minimum at $k_F < x < \pi/2$, the latter is correct at $\pi/2 < x < \pi - k_F$.
- $\pi - k_F < x < \pi \to -k/2 < v_- < L - 3k/2 - LQ/(2\pi)$. A true minimum corresponds to $\Delta E(Q) = 4\sin x \sin(-x - k_F)$

Appendix D

In this Appendix we list the formulas that determine the action of various hopping, creation and annihilation operators on states $\psi_{n_A}(n)$ and $\psi'_{n_A}(n')$. First remember the definition of our notation (31). In what follows the numbers n and n' are always given by

$$n = \sum_{j=1}^{n_A}\binom{p_j - 1}{j} \quad \text{and} \quad n' = \sum_{j=1}^{n_A-1}\binom{p_j-1}{j}, \quad \text{(D.1)}$$

First we consider the hopping term occurring in (8):

Hopping to the right $\tau_i^-\,\tau_{i+1}^+$

The matrix elements of the operator $\sum_{i=1}^{L}\tau_i^-\tau_{i+1}^+$ in the particle representation is non-zero whenever it is possible to move an $\mathscr{A}$-particle to the right. This means there has to be a $j\in\{1,\ldots,n_{\rm A}\}$ in such a way that $p_{j+1} > p_j + 1$, compare with (25). We have to take special care of the case $i = L-1$ or L (i.e. hopping to or from the periodic boundary), when an unprimed state transforms into a primed state and vice versa.

$i\in\{1,\ldots,L-2\}$, i.e. $p_{n_A} < L - n_A$

$$\psi_{n_A}(n) = |\cdots\mathscr{A}(p_j)\mathscr{B}\cdots\rangle \to \psi_{n_A}(m) = |\cdots\mathscr{B}\mathscr{A}(p_j+1)\cdots\rangle$$

$$m = n + \binom{p_j - 1}{j-1} \quad \text{(D.2)}$$

The same for a primed state $\psi_{n_A}{}'(n')$.

$i = L-1$, i.e. $p_{n_A} = L - n_A$:

$$\psi_{n_A}(n) = |\mathscr{B}\cdots\mathscr{A}\rangle \to \psi'_{n_A}(m') = |\cdots\mathscr{B}\mathscr{A}\rangle'$$

$$m' = \sum_{j=1}^{n_A-1}\binom{p_j-2}{j} \quad \text{(D.3)}$$

$i = L$, i.e. all primed states:

$$\psi'_{n_A}(n) = |\mathscr{B}\cdots\mathscr{A}\rangle' \to \psi_{n_A}(m) = |\mathscr{A}\cdots\mathscr{B}\rangle$$

$$m = \sum_{j=1}^{n_A-1}\binom{p_j-1}{j+1} \quad \text{(D.4)}$$

Hopping to the left $\tau_i^+\tau_{i+1}^-$

$i\in\{1,\ldots,L-2\}$, i.e. $p_{n_A} < L - n_A$:

$$\psi_{n_A}(n) = |\cdots\mathscr{B}\mathscr{A}(p_j)\cdots\rangle \to \psi_{n_A}(m) = |\cdots\mathscr{A}(p_j-1)\mathscr{B}\cdots\rangle$$

$$m = n - \binom{p_j-1}{j-1} \quad \text{(D.5)}$$

The same for a primed state $\psi'_{n_A}(n')$.

$i = L$, i.e. $p_1 = 1$:

$$\psi_{n_A}(n) = |\mathscr{A}\cdots\mathscr{B}\rangle \to \psi'_{n_A}(m') = |\mathscr{B}\cdots\mathscr{A}\rangle'$$

$$m' = \sum_{j=2}^{n_A} \binom{p_j - 1}{j - 1} \tag{D.6}$$

$i = L - 1$, i.e. all primed states:

$$\psi'_{n_A}(n') = |\cdots\mathscr{B}\mathscr{A}\rangle' \to \psi_{n_A}(m) = |\mathscr{B}\cdots\mathscr{A}\rangle$$

$$m = \binom{L - n_A - 1}{n} + \sum_{j=1}^{n_A - 1} \binom{p_j}{j} \tag{D.7}$$

Next we consider the creation and annihilation operators occurring in the complete model via (19). Again we have to take special care of the cases in which a domain wall at the bond linking site 1 and site L is created or annihilated.

Creation of domain walls $\tau_i^+ \tau_{i+2}^+$

The non-zero matrix elements of the operator $\sum_{i=1}^{L} \tau_i^+ \tau_{i+2}^+$ have to be determined via the rule (26). Let us denote with p_y a position between two successive $\mathscr{A}$-particles at positions p_x and p_{x+1} (with $p_{x+1} - p_x \geqq 4$) where a new pair of $\mathscr{A}$-particles can be created.

$p_y \in \{1, \ldots, n_A - 3\}$:

$$\begin{aligned}
&\psi_{n_A}(n) = |\mathscr{A}(p_1)\cdots\mathscr{A}(p_x)[\mathscr{B}(p_y)\mathscr{B}(p_y+1)\mathscr{B}(p_y+2)\\
&\quad \mathscr{B}(p_y+3)]\,\mathscr{A}(p_{x+1})\cdots\mathscr{A}(p_{n_A})\rangle\\
&\to \psi_{n_A}(m) = |\mathscr{A}(p_1)\cdots\mathscr{A}(p_x)\,\mathscr{A}(p_y)\mathscr{A}(p_y+1)\\
&\quad \mathscr{A}(p_{x+1}-2)\cdots\mathscr{A}(p_{n_A}-2)\rangle\\
&m = \sum_{j=1}^{x} \binom{p_j - 1}{j} + \binom{p_y - 1}{x+1} + \binom{p_y}{x}\\
&\qquad + \sum_{j=x+1}^{n_A} \binom{p_j - 3}{j+2}
\end{aligned} \tag{D.8}$$

The same for a primed state $\psi'_{n_A}(n')$ with n_A replaced by $n_A - 1$ in the last sum.

$p_y = L - n_A - 2$:

$$\psi_{n_A}(n) = |\mathscr{B}\mathscr{A}(p_1)\cdots\mathscr{A}(p_{n_A})\mathscr{B}\mathscr{B}\mathscr{B}\rangle$$

$$\to \psi'_{n_A}(m') = |\mathscr{A}(p_1 - 1)\cdots\mathscr{A}(p_{n_A} - 1)\mathscr{A}(L - n_A - 3)\mathscr{A}\rangle$$

$$m' = \sum_{j=1}^{n_A} \binom{p_j - 2}{j} + \binom{L - n_A - 4}{n_A + 1} \tag{D.9}$$

$p_y = L - n_A - 1$:

$$\psi_{n_A}(n) = |\mathscr{B}\mathscr{B}\mathscr{A}(p_1)\cdots\mathscr{A}(p_{n_A})\mathscr{B}\mathscr{B}\rangle$$

$$\to \psi_{n_A}(m) = |\mathscr{A}\mathscr{A}(p_1 - 1)\cdots\mathscr{A}(p_{n_A} - 1)\mathscr{A}\rangle$$

$$m = \sum_{j=1}^{n_A} \binom{p_j - 2}{j - 1} + \binom{L - n_A - 3}{n_A + 2} \tag{D.10}$$

$p_y = L - n_A$:

$$\psi_{n_A}(n) = |\mathscr{B}\mathscr{B}\mathscr{B}\,\mathscr{A}(p_1)\cdots\mathscr{A}(p_{n_A})\mathscr{B}\rangle$$

$$\to \psi'_{n_A}(m') = |\mathscr{A}(1)\mathscr{A}(p_1 - 2)\cdots\mathscr{A}(p_{n_A} - 2)\mathscr{A}\rangle'$$

$$m' = \sum_{j=1}^{n_A} \binom{p_j - 3}{j + 1} \tag{D.11}$$

Annihilation of domain walls $\tau_i^- \tau_{i+2}^-$

Now let there be two successive $\mathscr{A}$-particles at position p_x and $p_{x+1} = p_x + 1$, so that they can be annihilated by $\tau_i^- \tau_{i+2}^-$ for some suitably chosen i.

$p_x \in \{1, \ldots, L - n_A - 3\}$:

$$\begin{aligned}
&\psi_{n_A}(n) = |\mathscr{A}(p_1)\cdots\mathscr{A}(p_{x-1})\mathscr{A}(p_x)\mathscr{A}(p_x+1)\\
&\quad \times \mathscr{A}(p_{x+2}\cdots\mathscr{A}(p_{n_A})\rangle\\
&\to \psi_{n_A}(m) = |\mathscr{A}(p_1)\cdots\mathscr{A}(p_{x-1})\mathscr{B}(p_x)\mathscr{B}(p_x+1)\mathscr{B}(p_x+2)\\
&\quad \times \mathscr{B}(p_x+3)\,\mathscr{A}(p_{x+2}+2)\cdots\mathscr{A}(p_{n_A}+2)\rangle\\
&m = \sum_{j=1}^{x-1} \binom{p_j - 1}{j} + \sum_{j=x+2}^{n_A} \binom{p_j + 1}{j - 2}
\end{aligned} \tag{D.12}$$

The same for a primed state $\psi'_{n_A}(n')$ with n_A replaced by $n_A - 1$ in the last sum.

$p_x = L - n_A - 2$ for a primed state:

$$\psi'_{n_A}(n') = |\mathscr{A}(p_1)\cdots\mathscr{A}(p_{n_A-2})\,\mathscr{A}\mathscr{A}\rangle'$$

$$\to \psi_{n_A}(m) = |\mathscr{B}\,\mathscr{A}(p_1+1)\cdots\mathscr{A}(p_{n_A-2}+1)\,\mathscr{B}\mathscr{B}\mathscr{B}\rangle$$

$$m = \sum_{j=1}^{n_A - 2} \binom{p_j}{j} \tag{D.13}$$

$p_x = L - n_A - 1$ for an unprimed state:

$$\psi_{n_A}(n) = |\mathscr{A}\,\mathscr{A}(p_2)\cdots\mathscr{A}(p_{n_A-1})\,\mathscr{A}\rangle$$

$$\to \psi_{n_A}(m) = |\mathscr{B}\mathscr{B}\,\mathscr{A}(p_2+1)\cdots\mathscr{A}(p_{n_A-1}+1)\mathscr{B}\mathscr{B}\rangle$$

$$m = \sum_{j=2}^{n_A - 1} \binom{p_j}{j} \tag{D.14}$$

$p_x = L - n_A$ for a primed state:

$$\psi'_{n_A}(n') = |\mathscr{A}\,\mathscr{A}(p_2)\cdots\mathscr{A}(p_{n_A-1})\mathscr{A}\rangle'$$

$$\to \psi_{n_A}(m) = |\mathscr{B}\mathscr{B}\mathscr{B}\,\mathscr{A}(p_2+2)\cdots\mathscr{A}(p_{n_A-1}+2)\,\mathscr{B}\rangle$$

$$m = \sum_{j=2}^{n_A - 1} \binom{p_j - 1}{j} \tag{D.15}$$

In order to determine the non-zero matrix elements for creation/annihilation it is thus necessary to scan the whole particle configuration corresponding to $\psi(n)$ and to record the allowed values for x, y and p_x and p_y. An alternative technique would be to try to store the (very sparse) matrix for $\mathscr{H}_{\text{eff}}^{(2)}$. However, as in most cases, not the computational speed but the storage requirement is the limiting factor for the maximum possible system size.

References

1. Chakrabarti, B.K., Dutta, A., Sen P.: Quantum Ising Phases and Transitions in Transverse Ising Models, Lecture Notes in Physics **41** (1996); Sen, P., Chakrabarti, B.K.: Int. J. Mod. Phys. B **6**, 2439 (1992)
2. For an overview see: Sachdev S. in STATPHYS 19, Proceedings of the 19th IUPAP International Conference on Statistical Physics, Xiamen, China Hao, B.-L. (ed.) p. 289. Singapore: World Scientific 1996; Z. Phys. B **94**, 469 (1994)
3. Wu, W., Bitko, D., Rosenbaum T.F., Aeppli, G.: Phys. Rev. Lett. **71**, 1919 (1993); Rieger, H., Young, A.P.: Phys. Rev. Lett. **72**, 4141 (1994); Guo, M., Bhatt, R.N., Huse, D.: Phys. Rev. Lett. **72**, 4137 (1994); Thill, M.J., Huse, D.A.: Physica A, **15**, 321 (1995); Rieger, H., Young, A.P.: Phys. Rev. B, (in press 1996)
4. Selke, W.: Physics Reports **170**, 213 (1988)
5. Ioselevich, A.S., Capelmann, H.: Solid State Commun. **95**, 111 (1995); Ioselevich, A.S.: (unpublished)
6. Fisher, M.E., Selke, W., Phys. Rev. Lett. **44**, 1502 (1980)
7. Mattis, D.: The Theory of Magnetism II in Springer Series in Solid State Sciences Vol. 55, Fulde, P. Berlin Heidelberg: Springer 1985
8. Schulz, T.D., Mattis, D.C., Lieb, E.H.: Rev. Mod. Phys. **36**, 856 (1964)
9. Villain, J., Bak, P.: J. Physique **42**, 657 (1981)
10. Prokovsky, V.L., Talapov, A.L.: Sov. Phys. - JETP 48, 579 (1978)
11. Kosterlitz, J.M., Thouless, D.J.: J. Phys. C **6**, 1181 (1973)
12. For the infinite system it will be enough to check $k = 1$ and $k = N/2 - 1$, respectively, but for a periodic system we must use even k's
13. The criterium of relevancy of a perturbation which creates (annihilates) a p-"leg" dislocation is $p^2 < 8$. See, e.g., Coppersmith, S.N., Fisher, D., Halperin, B., Lee, P., Brinkman, W.: Phys. Rev. Lett. **46**, 549 (1981)
14. Hirsch, R.: Diploma-Thesis, University of Cologne 1988
15. Duxbury, P.M., Barber, M.N.: J. Phys. A **15**, 3219 (1982)